

## NUMERICAL ANALYSIS OF BIOLOGICAL TISSUE HEATING USING THE DUAL-PHASE LAG EQUATION WITH TEMPERATURE – DEPENDENT PARAMETERS

*Ewa Majchrzak, Mikołaj Stryczyński*

*Department of Computational Mechanics and Engineering, Silesian University of Technology  
Gliwice, Poland*

*ewa.majchrzak@polsl.pl, mikolaj.stryczyński@polsl.pl*

Received: 5 April 2022; Accepted: 7 September 2022

**Abstract.** The dual-phase lag equation is formulated for the case when the thermophysical parameters occurring in this equation are temperature-dependent. The axial-symmetrical domain of biological tissue heated by an external heat source is considered. The problem is solved using the implicit scheme of the finite difference method. At the stage of numerical computations, the analytical relationships taken from the literature describing changes in parameters are taken into account.

**MSC 2010:** 65Z05, 80M20

**Keywords:** bioheat transfer, dual-phase lag model, temperature-dependent parameters, finite difference method

### 1. Introduction

One of the methods supporting the treatment of lesions is tissue heating, i.e. artificially induced hyperthermia. Mathematical modeling allows one to support the planning of this type of treatment, e.g. by determining the temperature distribution in the analyzed tissues and estimating the degree of their destruction. There are various types of mathematical models that describe the heat flow in living tissues in the literature. These are the Pennes equation [1], the Cattaneo-Vernotte equation [2, 3], the dual-phase lag equation [4], the three-phase lag equation [5-7], models based on the theory of porous media [8] and models taking into account the presence of thermally significant blood vessels [9, 10]. In order to determine the values of thermophysical parameters present in these models, intensive experimental studies of various types of tissues are carried out [11, 12].

It should be noted that the heating of biological tissues changes their thermophysical properties. When the temperature rises to 80-99°C, both the thermal conductivity and volumetric specific heat increase [13-15], while the blood perfusion rate and

the metabolic heat source disappear [16]. Until now, in the modelling of artificial hyperthermia, the constant values of these parameters are usually adopted.

In this paper the temperature distribution in the domain of biological tissue heated by an external heat source is described by the dual-phase lag equation (DPLE). This equation is derived for the case of temperature-dependent thermophysical parameters and its form is essentially more complicated as in the case of the constant ones.

The problem is solved using the implicit scheme of the finite difference method. The calculations are also performed for constant and variable thermophysical parameters and on this basis the conclusions are formulated.

## 2. Dual-phase lag equation with temperature-dependent parameters

The dual-phase lag equation is based on the following relationship between the heat flux and the temperature gradient [4]

$$\mathbf{q}(X, t + \tau_q) = -\lambda(T) \text{grad}T(X, t + \tau_T) \quad (1)$$

where  $\mathbf{q}$  is the heat flux,  $T$  is the temperature,  $\lambda(T)$  is the thermal conductivity,  $\tau_q$  is the relaxation time, and  $\tau_T$  is the thermalization time,  $X$  denotes the spatial coordinates (e.g. in the cylindrical co-ordinate system  $X = \{r, \varphi, z\}$ ),  $t$  is the time.

The functions  $T$  and  $\mathbf{q}$  are expanded into the Taylor series with an accuracy to the first derivatives

$$\mathbf{q}(X, t) + \tau_q \frac{\partial \mathbf{q}(X, t)}{\partial t} = -\lambda(T) \text{grad}T(X, t) - \tau_T \lambda(T) \frac{\partial [\text{grad}T(X, t)]}{\partial t} \quad (2)$$

The well-known Fourier equation (a start point for further considerations) has the following form

$$c(T) \frac{\partial T(X, t)}{\partial t} = -\text{div} \mathbf{q}(X, t) + Q(X, t) \quad (3)$$

where  $c(T)$  is the volumetric specific heat and  $Q(X, t)$  is the source function. From the dependence (2) it follows

$$-\mathbf{q}(X, t) = \tau_q \frac{\partial \mathbf{q}(X, t)}{\partial t} + \lambda(T) \text{grad}T(X, t) + \tau_T \lambda(T) \frac{\partial [\text{grad}T(X, t)]}{\partial t} \quad (4)$$

Hence

$$-\text{div} \mathbf{q}(X, t) = \tau_q \frac{\partial \text{div} \mathbf{q}(X, t)}{\partial t} + \text{div} [\lambda(T) \text{grad}T(X, t)] + \tau_T \text{div} \left[ \lambda(T) \frac{\partial [\text{grad}T(X, t)]}{\partial t} \right] \quad (5)$$

Formula (5) is introduced into equation (3)

$$c(T) \frac{\partial T(X, t)}{\partial t} = \tau_q \frac{\partial \operatorname{div} \mathbf{q}(X, t)}{\partial t} + \operatorname{div}[\lambda(T) \operatorname{grad} T(X, t)] + \tau_T \operatorname{div} \left[ \lambda(T) \frac{\partial [\operatorname{grad} T(X, t)]}{\partial t} \right] + Q(X, t) \quad (6)$$

From equation (3) it follows that

$$\operatorname{div} \mathbf{q}(X, t) = -c(T) \frac{\partial T(X, t)}{\partial t} + Q(X, t) \quad (7)$$

This relationship is used in equation (6)

$$c(T) \frac{\partial T(X, t)}{\partial t} = \tau_q \frac{\partial}{\partial t} \left[ -c(T) \frac{\partial T(X, t)}{\partial t} + Q(X, t) \right] + \operatorname{div}[\lambda(T) \operatorname{grad} T(X, t)] + \tau_T \operatorname{div} \left[ \lambda(T) \frac{\partial [\operatorname{grad} T(X, t)]}{\partial t} \right] + Q(X, t) \quad (8)$$

that is

$$c(T) \frac{\partial T(X, t)}{\partial t} + \tau_q \frac{\partial}{\partial t} \left[ c(T) \frac{\partial T(X, t)}{\partial t} \right] = \operatorname{div}[\lambda(T) \operatorname{grad} T(X, t)] + \tau_T \operatorname{div} \left[ \lambda(T) \frac{\partial [\operatorname{grad} T(X, t)]}{\partial t} \right] + Q(X, t) + \tau_q \frac{\partial Q(X, t)}{\partial t} \quad (9)$$

The source function  $Q(X, t)$  is the sum of the component related to blood perfusion and metabolism

$$Q(X, t) = w(T) c_b [T_a - T(X, t)] + Q_{met}(T) \quad (10)$$

where  $w(T)$  is the blood perfusion rate,  $c_b$  is the specific heat of blood,  $T_a$  is the arterial blood temperature and  $Q_{met}(T)$  is the metabolic heat source.

### 3. Formulation of the problem

The axisymmetric biological tissue domain is considered ( $X = (r, z)$ ). The temperature field in the tissue is described by the dual-phase lag equation (9) in which

$$\operatorname{div}[\lambda(T) \operatorname{grad} T] = \frac{1}{r} \frac{\partial}{\partial r} \left( r \lambda(T) \frac{\partial T}{\partial r} \right) + \frac{\partial}{\partial z} \left( \lambda(T) \frac{\partial T}{\partial z} \right) \quad (11)$$

It is assumed that the surface  $0 \leq r \leq R$ ,  $z = 0$  is heated by the external heat flux

$$q_b = q_0 \frac{t}{t_e} \left( 1 - \frac{t}{t_e} \right) \exp \left( -\frac{r^2}{r_D^2} \right) \quad (12)$$

where  $q_0$  is the maximum heat flux,  $t_e$  is the exposure time, and  $r \leq r_D$ . On the remaining surfaces the no-flux condition  $q_b = 0$  is taken into account. It should be noted that in the dual-phase lag model the Neumann condition takes the form [17]

$$-\lambda(T) \left( \mathbf{n} \cdot \text{grad} T + \tau_T \mathbf{n} \cdot \text{grad} \frac{\partial T}{\partial t} \right) = q_b + \tau_q \frac{\partial q_b}{\partial t} \quad (13)$$

where  $\mathbf{n}$  is the normal outward vector and  $q_b$  is the known boundary heat flux.

The initial conditions are also known [17]

$$t = 0: \quad T = T_p, \quad \frac{\partial T}{\partial t} = \frac{Q(T_p)}{c(T_p)} \quad (14)$$

where  $T_p$  is the initial temperature of tissue.

In the case when the analytical formulas describing the dependencies of thermo-physical parameters on temperature are known, the equation (9) can be written as follows:

$$\begin{aligned} & \left\{ c(T) + \tau_q \left[ w(T) c_b - v(T) c_b (T_a - T) - P_{met}(T) \right] \right\} \frac{\partial T}{\partial t} + \\ & c(T) \tau_q \frac{\partial^2 T}{\partial t^2} + \tau_q \frac{dc(T)}{dT} \left( \frac{\partial T}{\partial t} \right)^2 = \text{div} [\lambda(T) \text{grad} T] + \\ & \tau_T \text{div} \left[ \lambda(T) \text{grad} \left( \frac{\partial T}{\partial t} \right) \right] + w(T) c_b (T_a - T) + Q_{met}(T) \end{aligned} \quad (15)$$

where  $v(T) = dw(T)/dT$ ,  $P_{met}(T) = dQ_{met}(T)/dT$  and

$$\begin{aligned} & \text{div} \left[ \lambda(T) \text{grad} T(r, z, t) \right] + \tau_T \text{div} \left[ \lambda(T) \text{grad} \frac{\partial T(r, z, t)}{\partial t} \right] = \\ & \frac{1}{r} \lambda(T) \left[ \frac{\partial T}{\partial r} + \tau_T \frac{\partial}{\partial r} \left( \frac{\partial T}{\partial t} \right) \right] + \frac{d\lambda(T)}{dT} \frac{\partial T}{\partial r} \left[ \frac{\partial T}{\partial r} + \tau_T \frac{\partial}{\partial r} \left( \frac{\partial T}{\partial t} \right) \right] + \\ & \lambda(T) \left[ \frac{\partial^2 T}{\partial r^2} + \tau_T \frac{\partial^2}{\partial r^2} \left( \frac{\partial T}{\partial t} \right) \right] + \frac{d\lambda(T)}{dT} \frac{\partial T}{\partial z} \left[ \frac{\partial T}{\partial z} + \tau_T \frac{\partial}{\partial z} \left( \frac{\partial T}{\partial t} \right) \right] + \\ & \lambda(T) \left[ \frac{\partial^2 T}{\partial z^2} + \tau_T \frac{\partial^2}{\partial z^2} \left( \frac{\partial T}{\partial t} \right) \right] \end{aligned} \quad (16)$$

#### 4. Temperature-dependent changes in tissue thermal properties

In the papers [13-15], the thermal properties of the liver, i.e. the thermal conductivity and the volumetric heat capacity measured as a function of temperature during the heating process, are presented.

Silva et al. [13] experimentally investigate the thermal properties of the ex vivo ovine liver in the hyperthermic temperature range, from 25 to 97°C and they proposed the following dependencies

$$\lambda(T) = 0.502 + 1.447 \cdot 10^{-11} \exp(0.256T) \left[ \frac{\text{W}}{\text{mK}} \right] \quad (17)$$

and

$$C(T) = 3.415 + 1.278 \cdot 10^{-12} \exp(0.289T) \left[ \frac{\text{MJ}}{\text{m}^3\text{K}} \right] \quad (18)$$

Moreover, the Authors also performed the thermal conductivity and volumetric specific heat measurements during the cooling process of the samples. It turns out that the values of the thermal properties decrease following the trend suggested by the models (17), (18), without showing any hysteresis phenomena. Thus, it is possible to observe that changes in thermal properties with high temperatures are reversible when complete vaporization of the tissue water content does not occur, i.e., when a temperature of 100°C is not reached. The tissue thermal properties return to their basal values during the cooling.

Mohammadi et al. [14] measured the thermal properties of the liver, pancreas and brain tissues in the temperature range from 22°C to around 97°C. Finally, the following approximations are proposed (a porcine liver)

$$\lambda(T) = 0.543 + 4.41 \cdot 10^{-10} \exp(0.222T) \left[ \frac{\text{W}}{\text{mK}} \right] \quad (19)$$

and

$$C(T) = 3.542 + 1.79 \cdot 10^{-10} \exp(0.233T) \left[ \frac{\text{MJ}}{\text{m}^3\text{K}} \right] \quad (20)$$

Lopresto et al. [15] for  $21^\circ\text{C} \leq T \leq 99^\circ\text{C}$  and a bovine liver suggest the dependencies

$$\lambda(T) = 0.5075 + 5.6261 \cdot 10^{-51} T^{25.296} \left[ \frac{\text{W}}{\text{mK}} \right] \quad (21)$$

and

$$C(T) = 3.3012 + \frac{3.6186}{100 - T} \left[ \frac{\text{MJ}}{\text{m}^3\text{K}} \right] \quad (22)$$

In Figures 1 and 2, the thermal conductivity (formulas (17), (19), (21)) and the volumetric specific heat (formulas (18), (20), (22)) as a function of temperature are shown.

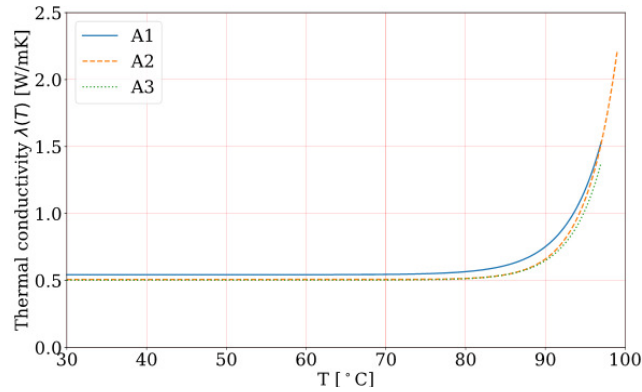


Fig. 1. Thermal conductivity as a function of temperature: A1 – formula (17), A2 – formula (19), A3 – formula (21)

As can be seen, these relationships do not differ much from each other, although they relate to the parameters of the liver for different animals. When analyzing these Figures, it can be seen that up to the temperature of 80°C, both the thermal conductivity and the volumetric specific heat hardly change. Hence the conclusion that in the case of modeling moderate hyperthermia, these parameters can be treated as the constant values. Above 90°C, a rapid increase in the values of the thermal conductivity and the volumetric specific heat is observed.

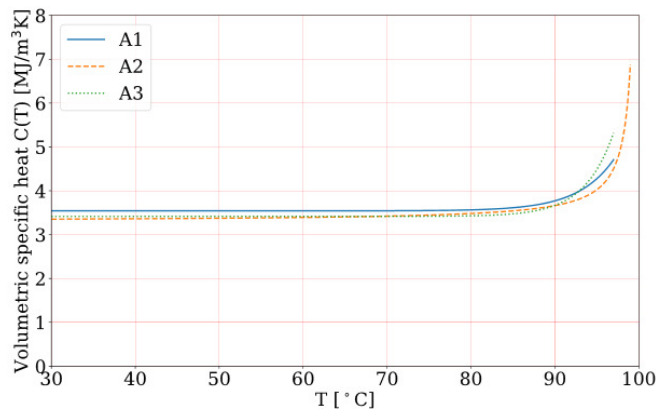


Fig. 2. Volumetric specific heat as a function of temperature: A1 – formula (18), A2 – formula (20), A3 – formula (22)

It should be noted that the blood perfusion rate  $w(T)$  and the metabolic heat source are also temperature dependent. A frequently used relationship that describes the change in blood perfusion rate versus temperature is [16]

$$w(T) = w_{b0} 2^{\frac{T-37}{10}} \quad (23)$$

where  $w_{b0}$  represents the basal blood perfusion rate. As can be seen, an increase in temperature of  $10^\circ\text{C}$  causes a two-fold increase in the blood perfusion rate compared to the initial value of  $w_{b0}$ .

A similar relationship is assumed for the metabolic heat source [16]

$$Q_{met}(T) = Q_{m0} 2^{\frac{T-37}{10}} \quad (24)$$

where  $Q_{m0}$  represents the basal metabolic heat source.

The relationships (23), (24) can be used to model the moderate hyperthermia in which the tissue temperature does not exceed  $50\text{-}55^\circ\text{C}$ . It is known that with further temperature increase, the metabolic component and blood perfusion rate gradually decrease to zero. Thus, in the computations presented later in this paper, due to the lack of experimental data, it was assumed that in the temperature range  $[55^\circ\text{C}, 90^\circ\text{C}]$  these components decrease linearly to zero.

## 5. Method of solution

To solve the problem formulated, the implicit scheme of the finite difference method is applied [10, 17]. The differential grid is shown in Figure 3.

For internal node  $(i, j)$ ,  $i = 1, 2, \dots, m-1, j = 1, 2, \dots, n-1$  and transition  $t^f \rightarrow t^{f+1}$  the following approximation of operator (16) is proposed

$$\begin{aligned} & \text{div} \left[ \lambda(T) \text{grad} T(r, z, t) \right]_{i,j}^{f+1} + \tau_T \text{div} \left[ \lambda(T) \text{grad} \frac{\partial T(r, z, t)}{\partial t} \right]_{i,j}^{f+1} = \\ & \frac{\lambda_{i,j}^f}{r_{i,j}} \left[ \frac{T_{i+1,j}^{f+1} - T_{i-1,j}^{f+1}}{2h} + \frac{\tau_T}{2h} \left[ \left( \frac{\partial T}{\partial t} \right)_{i+1,j}^{f+1} - \left( \frac{\partial T}{\partial t} \right)_{i-1,j}^{f+1} \right] \right] + \\ & \left( \frac{d\lambda(T)}{dT} \right)_{i,j}^f \frac{T_{i+1,j}^f - T_{i-1,j}^f}{2h} \left[ \frac{T_{i+1,j}^f - T_{i-1,j}^f}{2h} + \frac{\tau_T}{2h} \left[ \left( \frac{\partial T}{\partial t} \right)_{i+1,j}^f - \left( \frac{\partial T}{\partial t} \right)_{i-1,j}^f \right] \right] + \\ & \lambda_{i,j}^f \left[ \frac{T_{i-1,j}^{f+1} - 2T_{i,j}^{f+1} + T_{i+1,j}^{f+1}}{h^2} + \frac{\tau_T}{h^2} \left[ \left( \frac{\partial T}{\partial t} \right)_{i-1,j}^{f+1} - 2 \left( \frac{\partial T}{\partial t} \right)_{i,j}^{f+1} + \left( \frac{\partial T}{\partial t} \right)_{i+1,j}^{f+1} \right] \right] + \\ & \left( \frac{d\lambda(T)}{dT} \right)_{i,j}^f \frac{T_{i,j+1}^f - T_{i,j-1}^f}{2h} \left[ \frac{T_{i,j+1}^f - T_{i,j-1}^f}{2h} + \frac{\tau_T}{2h} \left[ \left( \frac{\partial T}{\partial t} \right)_{i,j+1}^f - \left( \frac{\partial T}{\partial t} \right)_{i,j-1}^f \right] \right] + \\ & \lambda_{i,j}^f \left[ \frac{T_{i,j-1}^{f+1} - 2T_{i,j}^{f+1} + T_{i,j+1}^{f+1}}{h^2} + \frac{\tau_T}{h^2} \left[ \left( \frac{\partial T}{\partial t} \right)_{i,j-1}^{f+1} - 2 \left( \frac{\partial T}{\partial t} \right)_{i,j}^{f+1} + \left( \frac{\partial T}{\partial t} \right)_{i,j+1}^{f+1} \right] \right] \end{aligned} \quad (25)$$

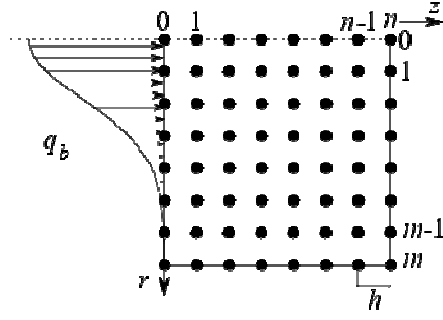


Fig. 3. Differential mesh

Next, the derivatives with respect to time are replaced by difference quotients, e.g.

$$\left(\frac{\partial T}{\partial t}\right)_{i,j}^{f+1} = \frac{T_{i,j}^{f+1} - T_{i,j}^f}{\Delta t} \quad (26)$$

where  $\Delta t$  is the time step.

After mathematical manipulations one has

$$\begin{aligned} \operatorname{div}[\lambda(T) \operatorname{grad} T(r, z, t)]_{i,j}^{f+1} + \tau_T \operatorname{div} \left[ \lambda(T) \operatorname{grad} \frac{\partial T(r, z, t)}{\partial t} \right]_{i,j}^{f+1} = \\ A_{i,j}^f \left( 1 - \frac{h}{2r_{i,j}} \right) T_{i-1,j}^{f+1} + A_{i,j}^f \left( 1 + \frac{h}{2r_{i,j}} \right) T_{i+1,j}^{f+1} + A_{i,j}^f (T_{i,j-1}^{f+1} + T_{i,j+1}^{f+1}) - 4A_{i,j}^f T_{i,j}^{f+1} + B_{i,j}^f \end{aligned} \quad (27)$$

where

$$A_{i,j}^f = \frac{\lambda_{i,j}^f (\Delta t + \tau_T)}{h^2 \Delta t} \quad (28)$$

and

$$\begin{aligned} B_{i,j}^f = -\frac{\lambda_{i,j}^f \tau_T}{h^2 \Delta t} (T_{i-1,j}^f + T_{i+1,j}^f + T_{i,j-1}^f + T_{i,j+1}^f - 4T_{i,j}^f) - \frac{\lambda_{i,j}^f \tau_T}{2hr_{i,j} \Delta t} (T_{i+1,j}^f - T_{i-1,j}^f) + \\ \frac{1}{4h^2 \Delta t} \left( \frac{d\lambda(T)}{dT} \right)_{i,j}^f \left[ (\Delta t + \tau_T) (T_{i+1,j}^f - T_{i-1,j}^f)^2 - \tau_T (T_{i+1,j}^f - T_{i-1,j}^f) (T_{i+1,j}^{f-1} - T_{i-1,j}^{f-1}) \right] + \\ \frac{1}{4h^2 \Delta t} \left( \frac{d\lambda(T)}{dT} \right)_{i,j}^f \left[ (\Delta t + \tau_T) (T_{i,j+1}^f - T_{i,j-1}^f)^2 - \tau_T (T_{i,j+1}^f - T_{i,j-1}^f) (T_{i,j+1}^{f-1} - T_{i,j-1}^{f-1}) \right] \end{aligned} \quad (29)$$

The approximation of the left-hand side of equation (15) is as follows

$$\begin{aligned}
 & \left\{ c(T) + \tau_q \left[ w(T)c_b - v(T)c_b(T_a - T) - P_{met}(T) \right] \right\}_{i,j}^{f+1} \left( \frac{\partial T}{\partial t} \right)_{i,j}^{f+1} + \\
 & \tau_q \left( c(T) \frac{\partial^2 T}{\partial t^2} \right)_{i,j}^{f+1} + \tau_q \left[ \frac{dc(T)}{dT} \left( \frac{\partial T}{\partial t} \right)^2 \right]_{i,j}^{f+1} = \\
 & \left\{ c_{i,j}^f + \tau_q \left[ w_{i,j}^f c_b - v_{i,j}^f c_b (T_a - T_{i,j}^f) - (P_{met})_{i,j}^f \right] \right\} \frac{T_{i,j}^{f+1} - T_{i,j}^f}{\Delta t} + \\
 & \tau_q c_{i,j}^f \frac{T_{i,j}^{f+1} - 2T_{i,j}^f + T_{i,j}^{f-1}}{(\Delta t)^2} + \tau_q \left( \frac{dc(T)}{dT} \right)_{i,j}^f \left( \frac{T_{i,j}^f - T_{i,j}^{f-1}}{\Delta t} \right)^2
 \end{aligned} \tag{30}$$

The following approximation of equation (15) is obtained

$$\begin{aligned}
 & \left\{ c_{i,j}^f + \tau_q \left[ w_{i,j}^f c_b - v_{i,j}^f c_b (T_a - T_{i,j}^f) - (P_{met})_{i,j}^f \right] \right\} \frac{T_{i,j}^{f+1} - T_{i,j}^f}{\Delta t} + \\
 & \tau_q c_{i,j}^f \frac{T_{i,j}^{f+1} - 2T_{i,j}^f + T_{i,j}^{f-1}}{(\Delta t)^2} + \tau_q \left( \frac{dc(T)}{dT} \right)_{i,j}^f \left( \frac{T_{i,j}^f - T_{i,j}^{f-1}}{\Delta t} \right)^2 = \\
 & A_{i,j}^f \left( 1 - \frac{h}{2r_{i,j}} \right) T_{i-1,j}^{f+1} + A_{i,j}^f \left( 1 + \frac{h}{2r_{i,j}} \right) T_{i+1,j}^{f+1} + A_{i,j}^f (T_{i,j-1}^{f+1} + T_{i,j+1}^{f+1}) - \\
 & 4A_{i,j}^f T_{i,j}^{f+1} - w_{i,j}^f c_b T_{i,j}^{f+1} + D_{i,j}^f
 \end{aligned} \tag{31}$$

where

$$D_{i,j}^f = B_{i,j}^f + w_{i,j}^f c_b T_a + (Q_{met})_{i,j}^f \tag{32}$$

Equation (31) can be converted to the form

$$T_{i,j}^{f+1} = \frac{A_{i,j}^f}{F_{i,j}^f} \left( 1 - \frac{h}{2r_{i,j}} \right) T_{i-1,j}^{f+1} + \frac{A_{i,j}^f}{F_{i,j}^f} \left( 1 + \frac{h}{2r_{i,j}} \right) T_{i+1,j}^{f+1} + \frac{A_{i,j}^f}{F_{i,j}^f} (T_{i,j-1}^{f+1} + T_{i,j+1}^{f+1}) + \frac{E_{i,j}^f}{F_{i,j}^f} \tag{33}$$

where

$$\begin{aligned}
 E_{i,j}^f = D_{i,j}^f + & \frac{\left\{ c_{i,j}^f + \tau_q \left[ w_{i,j}^f c_b - v_{i,j}^f c_b (T_a - T_{i,j}^f) - (P_{met})_{i,j}^f \right] \right\} \Delta t + 2\tau_q c_{i,j}^f}{(\Delta t)^2} T_{i,j}^f - \\
 & \frac{c_{i,j}^f \tau_q}{(\Delta t)^2} T_{i,j}^{f-1} - \tau_q \left( \frac{dc(T)}{dT} \right)_{i,j}^f \left( \frac{T_{i,j}^f - T_{i,j}^{f-1}}{\Delta t} \right)^2
 \end{aligned} \tag{34}$$

and

$$F_{i,j}^f = \frac{\left\{ c_{i,j}^f + \tau_q \left[ w_{i,j}^f c_b - v_{i,j}^f c_b (T_a - T_{i,j}^f) - (P_{met})_{i,j}^f \right] \right\} \Delta t + \tau_q c_{i,j}^f + w_{i,j}^f c_b (\Delta t)^2}{(\Delta t)^2} + 4A_{i,j}^f \quad (35)$$

The differential approximation of the boundary condition (13) is as follows

$$-\lambda_{i,j}^f \left[ (\mathbf{n} \cdot \text{grad } T)_{i,j}^{f+1} + \frac{\tau_T}{\Delta t} \left[ (\mathbf{n} \cdot \text{grad } T)_{i,j}^{f+1} - (\mathbf{n} \cdot \text{grad } T)_{i,j}^f \right] \right] = q_b + \tau_q \frac{\partial q_b}{\partial t} \quad (36)$$

For  $j = 0$  ( $i = 1, 2, \dots, m-1$ ) one obtains

$$T_{i,j}^{f+1} = T_{i,j+1}^{f+1} - \frac{\tau_T}{\Delta t + \tau_T} (T_{i,j+1}^f - T_{i,j}^f) + \frac{h \Delta t}{\lambda_{i,j}^f (\Delta t + \tau_T)} \left[ (q_b)_{i,j}^{f+1} + \tau_q \left( \frac{\partial q_b}{\partial t} \right)_{i,j}^{f+1} \right] \quad (37)$$

Equations for the remaining boundary nodes are obtained in a similar way.

For the transition  $t^f \rightarrow t^{f+1}$ , the system of equations (33) is solved using the iterative method. The iterative process has been continued until the condition  $\left| (T_{i,j}^{f+1})^k - (T_{i,j}^{f+1})^{k-1} \right| \leq \varepsilon$  for each node has been fulfilled, where  $k$  is the number of iterations. It should be noted that the presented algorithm is unconditionally stable [18].

## 6. Results of computations

The cylindrical fragment of the tissue domain ( $R = 0.02$  m,  $Z = 0.02$  m) is considered. The surface  $0 \leq r \leq R, z = 0$  is heated by the external heat flux (formula (12)) where  $q_0 = 53$  kW/m<sup>2</sup> is the maximum heat flux,  $t_e = 120$  s is the exposure time,  $r_D = 0.005$  m and  $r \leq r_D$ . On the remaining surfaces the no-flux condition  $q_b = 0$  is taken into account. The initial tissue temperature is equal to  $T_p = 37^\circ\text{C}$ , arterial blood temperature equals  $T_a = 37^\circ\text{C}$  and specific heat of blood equals  $c_b = 3770$  J/(kg K).

At the beginning, the computations were performed assuming constant thermal properties of the tissue, namely thermal conductivity  $\lambda = \lambda(T_p)$  (equation (17)), volumetric specific heat  $c = c(T_p)$  (equation (18)), blood perfusion rate  $w = w(T_p) = w_{b0} = 0.5$  kg/(m<sup>3</sup>s) (equation (23)), metabolic heat source  $Q_{met} = Q_{met}(T_p) = Q_{m0} = 245$  W/m<sup>3</sup> (equation (24)), relaxation time  $\tau_q = 4$  s, and thermalization time  $\tau_T = 2$  s [8, 10].

The problem is solved using the implicit scheme of the finite difference method under the assumption that  $n = m = 100$  (grid step is equal to  $h = 0.0002$  m), and the time step is equal to  $\Delta t = 0.0005$  s. The computations are also done for  $n = 50$  and

$n = 150$ , and it turns out that  $n = 100$  ensures the fine-enough mesh-size needed to generate accurate results. A small-time step is assumed to ensure a good approximation of the changes in the boundary heat flux (12) and the temperature-dependent values of tissue parameters.

Next, the problem is solved using temperature-dependent parameters (equations (17), (18), (23), (24)). Figure 4 shows the temperature history at the points A(0.0002 m, 0), B(0.004 m, 0) for constant and temperature-dependent parameters.

As expected, in the initial stage of the process, these curves coincide, because the values of  $\lambda(T)$  and  $C(T)$  for lower temperatures are almost constant (see: Figures 1 and 2), and the other parameters  $w(T)$  and  $Q_{met}(T)$  have a little influence on the temperature values. Significant differences appear when the temperature rises above  $90^{\circ}\text{C}$ , and they are about  $6^{\circ}\text{C}$ . In the case of constant parameters, the temperature is larger. During the cooling stage, the differences decrease.

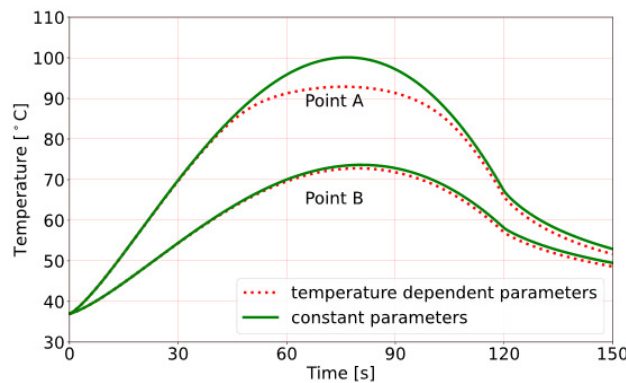


Fig. 4. Temperature courses at points A and B for constant and temperature-dependent tissue parameters

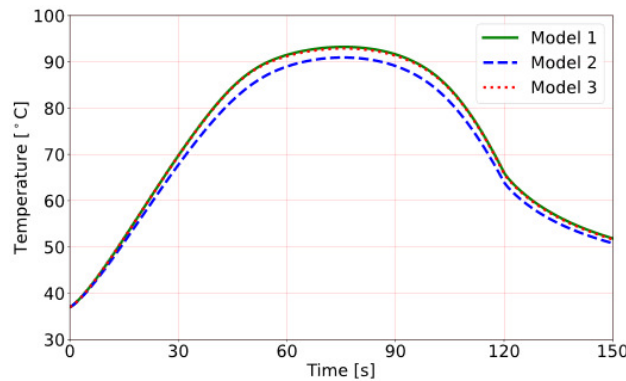


Fig. 5. Temperature courses at point A, Model 1 – equations (17), (18); Model 2 – equations (19), (20); Model 3 – equations (21), (22)

The computations are also performed for the set of equations (19)-(20) and (21)-(22). In Figure 5 the temperature courses at the point A are presented. Model 1

concerns the ovine liver (equations (17)-(18)), model 2 concerns the porcine liver (equations (19)-(20)), while model 3 concerns the bovine liver (equations (21)-(22)). It is visible that the curves corresponding to the models 1 and 3 almost match. Slightly lower temperatures are obtained for model 2 (Table 1).

Table 1. Maximum temperatures

	Model 1	Model 2	Model 3	$S$
Max temperature [°C]	93.226	90.941	92.892	1.008

The aim of the next computations is to estimate the influence of the delay times values  $\tau_q$  and  $\tau_T$  on the temperature distributions (Fig. 6). The results of the simulations are listed in Table 2.

In Tables 1 and 2 information about the values of standard deviations  $S$  with respect to the mean values is also presented.

Table 2. Temperatures at point A calculated for different time delays

Time delays [s]	$\tau_T = 2, \tau_q = 4$	$\tau_T = 0, \tau_q = 4$	$\tau_T = 10, \tau_q = 14$	$\tau_T = 0.1, \tau_q = 1$	$S$
Time [s]	Temperature [°C]				
60	91.234	91.533	93.382	90.709	1.007
90	91.332	91.420	90.855	91.596	0.274
120	65.832	64.773	63.137	66.888	1.386
150	51.672	51.133	50.133	51.922	0.687

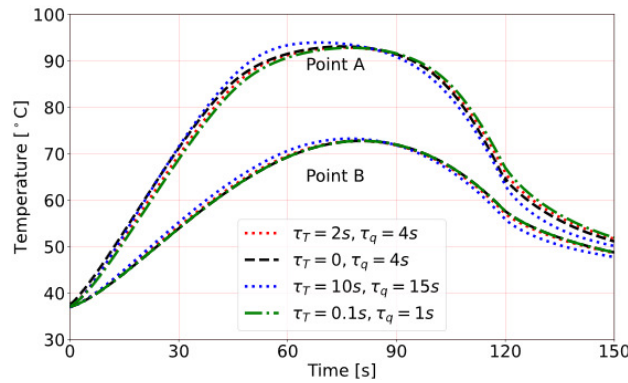


Fig. 6. Temperature courses at points A and B for different values of time delays  $\tau_q$  and  $\tau_T$

## 7. Conclusions

The dual-phase lag equation for temperature-dependent thermophysical parameters of biological tissue has been formulated. The DPLE supplemented by appropriate

boundary and initial conditions has been solved using the implicit scheme of the finite difference method.

The performed computations showed that in the case of temperatures reaching 80-99°C, there are significant differences in temperature distributions for variable and constant thermophysical parameters. The differences in the temperature distributions caused by different values of the delay times are smaller and do not exceed 1%.

Hence the conclusion that in the modelling of high-temperature hyperthermia, the variability of thermophysical parameters with temperature should be considered.

### Acknowledgement

The research is financed from financial resources from the statutory subsidy of the Faculty of Mechanical Engineering, Silesian University of Technology in 2022.

### References

- [1] Pennes, H.H. (1948). Analysis of tissue and arterial blood temperatures in the resting human forearm. *Journal of Applied Physiology*, 1, 93-122.
- [2] Cattaneo, M.C. (1958). A form of heat conduction equation which eliminates the paradox of instantaneous propagation. *Compte Rendus*, 247, 431-433.
- [3] Vernotte, P. (1958). Les paradoxes de la theorie continue de l'equation de la chaleur. *Compte Rendus*, 246, 3154-3155.
- [4] Tzou, D.Y. (1996). *Macro- to Microscale Heat Transfer: The Lagging Behavior*. Washington, DC: Taylor and Francis.
- [5] Choudhuri, S.R. (2007). On a thermoelastic three-phase-lag model. *Journal of Thermal Stresses*, 30, 231-238.
- [6] Singh, S., Saccomandi, P., & Melnik, R. (2022). Three-phase-lag bio-heat transfer model of cardiac ablation. *Fluids*, 7(180) (15pp).
- [7] Kumar, D., & Rai, K.N. (2022). Three-phase-lag bioheat transfer model and its validation with experimental data. *Mechanics Based Design of Structures and Machines*, 50(7), 2493-2507.
- [8] Zhang, Y. (2009). Generalized dual-phase lag bioheat equations based on nonequilibrium heat transfer in living biological tissues. *International Journal of Heat and Mass Transfer*, 52, 4829-4834.
- [9] Jamshidi, M., & Ghazanfarian, J. (2021). Blood flow effects in thermal treatment of three-dimensional non-Fourier multilayered skin structure. *Heat Transfer Engineering*, 42(11), 929-946.
- [10] Majchrzak, E., & Stryczyński, M. (2021). Dual-phase lag model of heat transfer between blood vessel and biological tissue. *Mathematical Biosciences and Engineering*, 18(2), 1573-1589.
- [11] Bianchi, L., Cavarzan, F., Ciampitti, L., Cremonesi, M., Grilli, F., & Saccomandi, P. (2022). Thermophysical and mechanical properties of biological tissues as a function of temperature: a systematic literature review. *International Journal of Hyperthermia*, 39(1), 297-340.
- [12] Rossmann, Ch., & Haemmerich, D. (2014). Review of temperature dependence of thermal properties, dielectric properties, and perfusion of biological tissues at hyperthermic and ablation temperatures. *Critical Reviews in Biomedical Engineering*, 42(6), 467-492.

- 
- [13] Silva, N.P., Bottiglieri, A., Conceição, R.C., O'Halloran, M., & Farina, L. (2020). Characterisation of ex vivo liver thermal properties for electromagnetic-based hyperthermic therapies. *Sensors*, 20, 3004 (14pp).
  - [14] Mohammadi, A., Bianchi, L., Asadi, S., & Saccomandi, P. (2021). Measurement of ex vivo liver, brain and pancreas thermal properties as function of temperature. *Sensors*, 21, 4236 (15pp).
  - [15] Lopresto, V., Argentieri, A., Pinto, R., & Cavagnaro, (2019). Temperature dependence of thermal properties of ex vivo liver tissue up to ablative temperatures. *Physics in Medicine & Biology*, 105016 (15pp).
  - [16] Iljaž, J., Wrobel, L.C., Hriberšek, M., & Marn, J. (2019). Numerical modelling of skin tumour tissue with temperature-dependent properties for dynamic thermography. *Computers in Biology and Medicine*, 112, 103367 (15pp).
  - [17] Majchrzak, E., & Kałuża, G. (2022). Sensitivity analysis of temperature in heated soft tissues with respect to time delays. *Continuum Mechanics and Thermodynamics*, 34, 587-599.
  - [18] Majchrzak, E., & Mochnacki, B. (2017). Implicit scheme of the finite difference method for 1D dual-phase lag equation. *Journal of Applied Mathematics and Computational Mechanics*, 16(3), 37-46.